

Downregulation of microRNA-100/microRNA-125b is associated with lymph node metastasis in early colorectal cancer with submucosal invasion

Yasuteru Fujino,¹ Shunsaku Takeishi,¹ Kensei Nishida,² Koichi Okamoto,¹ Naoki Muguruma,¹ Tetsuo Kimura,¹ Shinji Kitamura,¹ Hiroshi Miyamoto,¹ Akiko Fujimoto,¹ Jun Higashijima,³ Mitsuo Shimada,³ Kazuhito Rokutan² and Tetsuji Takayama¹

¹Department of Gastroenterology and Oncology, Institute of Biomedical Sciences, Tokushima University Graduate School, Tokushima; ²Department of Pathophysiology, Institute of Biomedical Sciences, Tokushima University Graduate School, Tokushima; ³Department of Surgery, Institute of Biomedical Sciences, Tokushima University Graduate School, Tokushima, Japan

Key words

Cancer invasion, colorectal cancer with submucosal invasion, lymph node metastasis, miR-100, miR-125b

Correspondence

Tetsuji Takayama, Department of Gastroenterology and Oncology, Institute of Biomedical Biosciences, The University of Tokushima Graduate School, 3-18-15, Kuramoto-cho, Tokushima City 770-8503, Japan.
Tel: +81-88-633-7122; Fax: +81-88-633-9235;
E-mail: takayama@tokushima-u.ac.jp

Funding Information

Japan Society for the Promotion of Science (15K09059); Japanese Foundation for Research and Promotion of Endoscopy.

Received August 24, 2016; Revised December 21, 2016; Accepted December 25, 2016

Cancer Sci 108 (2017) 390–397

doi: 10.1111/cas.13152

A majority of early colorectal cancers (CRCs) with submucosal invasion undergo surgical operation, despite a very low incidence of lymph node metastasis. Our study aimed to identify microRNAs (miRNAs) specifically responsible for lymph node metastasis in submucosal CRCs. MicroRNA microarray analysis revealed that miR-100 and miR-125b expression levels were significantly lower in CRC tissues with lymph node metastases than in those without metastases. These results were validated by quantitative real-time PCR in a larger set of clinical samples. The transfection of a miR-100 or miR-125b inhibitor into colon cancer HCT116 cells significantly increased cell invasion, migration, and MMP activity. Conversely, overexpression of miR-100 or miR-125b mimics significantly attenuated all these activities but did not affect cell growth. To identify target mRNAs, we undertook a gene expression array analysis of miR-100-silenced HCT116 cells as well as negative control cells. The Ingenuity Pathway Analysis, TargetScan software analyses, and subsequent verification of mRNA expression by real-time PCR identified mammalian target of rapamycin (mTOR) and insulin-like growth factor 1 receptor (IGF1R) as direct, and Fas and X-linked inhibitor-of-apoptosis protein (XIAP) as indirect candidate targets for miR-100 involved in lymph node metastasis. Knockdown of each gene by siRNA significantly reduced the invasiveness of HCT116 cells. These data clearly show that downregulation of miR-100 and miR-125b is closely associated with lymph node metastasis in submucosal CRC through enhancement of invasion, motility, and MMP activity. In particular, miR-100 may promote metastasis by upregulating mTOR, IGF1R, Fas, and XIAP as targets. Thus, miR-100 and miR-125b may be novel biomarkers for lymph node metastasis of early CRCs with submucosal invasion.

Recent advances in endoscopic technology enable us to correctly diagnose relatively early CRCs. At the same time, with the development of endoscopic therapies, including endoscopic mucosal resection and endoscopic submucosal dissection, we are now able to completely remove en bloc CRCs with limited invasion to the superficial submucosal layer.⁽¹⁾ However, it has been reported that approximately 10% of CRCs with submucosal invasion metastasize to lymph nodes.⁽²⁾ In the absence of lymph node metastasis, CRCs with submucosal invasion could be cured by endoscopic treatment alone. However, surgical operation with lymph node resection is commonly carried out to treat CRCs with submucosal invasion, as we have no reliable diagnostic method to detect small lymph node metastasis. In fact, the Japanese and European guidelines recommend surgical resection when the CRC infiltrates into the deep submucosal layer (>1 mm).^(3,4) The US guideline recommends surgical resection for CRC with submucosal invasion, regardless of the depth of submucosal

invasion.⁽⁵⁾ However, lymph node metastases are rarely detected in resected tissues from surgical operations. Considering these clinical circumstances, the development of novel biomarkers specifically related to lymph node metastasis is very important for the treatment of CRCs with submucosal invasion.

MicroRNAs are a class of small non-coding RNA molecules of 20–25 nt that regulate gene expression through transcriptional repression and mRNA degradation.^(6–10) Accumulating evidence has shown that miRNAs are involved in carcinogenesis, metastasis, and invasion in various types of cancers.^(11,12) Moreover, the recent development of miRNA microarray assay has made possible to evaluate the expression of >3000 miRNAs simultaneously.⁽¹³⁾ Using this method, several studies detected miRNAs responsible for metastasis of human CRCs. Li *et al.*⁽¹⁴⁾ showed that decreased miR-99b expression in metastatic lesions of the liver from CRCs promoted cell invasion through enhancement of mTOR expression. Yuan *et al.*⁽¹⁵⁾

reported that miR-145 expression was significantly higher in CRC with lymph node metastasis than in CRC without lymph node metastasis, and showed that forced expression of miR-145 enhanced invasion and metastasis of HCT-8 cells through stabilization of heat shock protein-27 mRNA. Conversely, it was reported that miR-145 expression was decreased in lung cancer with lymph node metastasis.^(16,17) However, these reports mainly focused on advanced CRCs (stage III and IV), and early CRCs with submucosal invasion were not investigated.

In our study, by analyzing miRNA expression profiles in submucosal invasive CRCs with and without lymph node metastasis, we identified miR-100 and miR-125b as possible miRNAs useful for risk assessment of lymph node metastasis in CRC. We also identified their target genes, which facilitate invasion and migration of CRC cells.

Materials and Methods

Tissue specimens. We enrolled six patients with submucosal invasive CRC with lymph node metastasis and 10 patients with submucosal invasive CRC without lymph node metastasis. Baseline characteristics of the patients are shown in Table S1. Specimens were obtained by endoscopic mucosal resection or surgical removal, fixed in 10% formalin, and embedded in paraffin. Written informed consent was obtained from all patients according to the guidelines approved by the Ethics Committee of Tokushima University Hospital (approval no. 1318-1).

Cell lines. Human CRC cell lines (HT29, SW480, RKO, and HCT116) were purchased from ATCC (Manassas, VA, USA). COLO 205 was purchased from RIKEN Cell Bank (Kobe, Japan). HT29 and HCT116 cells were cultured in McCoy's 5A medium containing 10% FBS, SW480 cells were cultured in Leibovitz's L-15 medium containing 10% FBS, RKO cells were cultured in the Minimum Essential Medium Eagle containing 10% FBS, and COLO 205 cells were cultured in RPMI-1640 medium containing 10% FBS.

MicroRNA microarray. After macrodissection of 20- μ m CRC tissue slices, total RNA was extracted using a miRNeasy FFPE Kit (Qiagen, Hilden, Germany). A human miRNA microarray (version 3, based on Sanger miRbase release 12.0; Agilent Technologies, Palo Alto, CA, USA) was used for measuring global miRNA expression in CRC samples. Total RNA was labeled with cyanine 3-cytidine bisphosphate by T4 ligase and hybridized to SurePrint G3 human miRNA microarray release 16.0 using miRNA complete labeling reagent and hybridization kit (Agilent Technologies). Subsequently, each sample was scanned by a DNA Microarray Scanner (G2505C; Agilent Technologies), and fluorescence signal was extracted using Feature Extraction Software (version 10.7.3.1). Raw intensity miRNA data were analyzed by GeneSpring GX 12 (Agilent Technologies).

Gene expression and pathway analyses. Total RNA was extracted from HCT116 cells using an RNeasy Mini Kit (Qiagen). The quality of the purified RNA was assessed, and gene expression was measured using a whole human genome microarray (SurePrint G3 Human GE 8x 60K; Agilent Technologies) as described previously.⁽¹⁸⁾ Microarray data were analyzed by GeneSpring GX 12. The functional pathways related to the set of differentially expressed genes were assessed by IPA (<http://www.ingenuity.com>). TargetScan (<http://www.targetscan.org/>) was also used to predict the target of miRNA.

TaqMan real-time RT-PCR. Total RNA was extracted from human CRC tissues as described above. Mature miRNA levels were measured using TaqMan MicroRNA Assays (Applied Biosystems, Foster City, CA, USA). RNU48 snRNA was used as an internal quantity control for normalization. The following TaqMan microRNA assays reagents (Applied Biosystems) were used: hsa-miR-100 (000437), hsa-miR-125a-5p (002198), hsa-miR-125b (000449), hsa-miR-155 (002623), hsa-miR-30a-5p (000417), hsa-miR-342-3p (002260), and RNU48 (001006).

Total RNA was also extracted from HCT116 cells using an RNeasy Mini Kit. Amounts of mRNAs were measured by TaqMan qPCR and normalized by 18S ribosomal RNA (18S rRNA) using the following TaqMan primer sets (Applied Biosystems): *mTOR* (Hs00234522_m1), *IGF1R* (Hs00609566_m1), *Fas* (Hs00181225_m1), XIAP (Hs00745222_s1), and 18S rRNA (Hs03928985_g1). The relative expression levels of each sample were measured by the $2^{-\Delta\Delta C_T}$ method.

Overexpression or knockdown experiments. A specific inhibitor for miR-100 or miR-125b (mirVana miRNA Inhibitor; Life Technologies, Karlsruhe, Germany) was used for knockdown experiments, and a miR-100 or miR-125b mimic (mirVana miRNA mimic; Life Technologies) was used for overexpression experiments. HCT116 cells (14.4×10^5) were plated in 60-mm diameter dishes and transfected with one of the two inhibitors or mimics at a final concentration of 30 nM using the Lipofectamine RNAiMAX (Invitrogen, Carlsbad, CA, USA) in Opti-MEM medium (Gibco Life Technologies, Gaithersburg, MD, USA). A miRNA inhibitor negative control (mirVana miRNA inhibitor, negative control #1; Life Technologies) or miRNA mimic negative control (mirVana miRNA mimic, negative control #1; Life Technologies) was transfected as the respective negative control. HCT116 cells were transfected with 30 nM siRNA targeting *mTOR* (Silencer Select s604; Ambion, Austin, TX, USA) (sense, GGAGCCUUGUUGAUCCUATT; antisense, UAAGGAUCAACAAGGCUCCAT), *IGF1R* (Silencer Select s7211; Ambion) (sense, GCAUGGUAGCCGAAGAUUUTT; antisense, AAAUCUUCGGCUACCAUGCAA), *Fas* (Silencer Select s1506; Ambion) (sense, GGAAGACUGUACUACAGUTT; antisense, ACUGUAGUAACAGUCUUCCTC), and XIAP (Silencer Select s1454; Ambion) (sense, GGAUAUACUCAGUUAACAATT; antisense, UUGUUAACUGAGUUAUCCAT) using Lipofectamine RNAiMAX. A scramble siRNA (Silencer Negative Control #1, AM4611; Ambion) was used as a control siRNA.

Cell invasion assay. After transfection with the miRNA inhibitor, miRNA mimic, or siRNA, the cells were starved in serum-free media for 16 h. Subsequently, the *in vitro* invasion assay was carried out using the CultreCoat 96-well BME Cell Invasion Assay Kit (Trevigen, Gaithersburg, MD, USA) as previously described.⁽¹⁹⁾ Experiments were carried out six times.

Wound healing assay. Cells (2.0×10^6 cells) were transfected with miRNA inhibitor or miRNA mimic for 24 h in six-well plates. The confluent cell layer was scratched using a 200- μ L pipette tip, gently washed with PBS, and incubated in the culture medium containing 10% FBS. Wound healing was imaged every 30 min for 48 h using BioStation CT (Nikon, Tokyo, Japan). Wound healing ability was determined by measuring the migration distance in five points per sample at 16 h after the scratch.

Matrix metalloproteinase activity and cell proliferation assays. Cells were transfected with miRNA inhibitors or mimics in 60-mm diameter dishes for 24 h. After washing, they were incubated with fresh medium for 24 h, and the conditioned

medium was collected. Matrix metalloproteinase activities (MMP-1, 2, 7, 8, 9, 13, 14, 15, and 16) were measured using the Sensolyte 390 generic MMP activity kit (AnaSpec, Fremont, CA, USA) as previously described.⁽²⁰⁾ For the proliferation assay, after transfection with a miRNA inhibitor or mimic, cells (3.0×10^3) were plated in a 96-well plate and incubated in McCoy's 5A medium with 10% FBS. Viable cells were counted at 6, 24, 48, 72, 96, and 120 h using a Cell Counting Kit-8 (Dojindo Laboratories, Kumamoto, Japan).

Statistical analysis. The unpaired *t*-test was used to assess difference in miRNA array expression between human CRC tissues with and without lymph node metastasis. The Mann–Whitney *U*-test was used to assess difference in real-time PCR expression between human CRC tissues with and without lymph node metastasis. Dunnett's test was used to assess difference in invasion, proliferation, and MMP activity between control cells and cells transfected with miRNA inhibitors, mimics, or siRNAs. In the network analysis using the IPA system, the probability of a relationship between each biological function and the identified genes was calculated by the Fisher's exact test. The level of significance was set at a *P*-value of 0.05.

Results

Differentially expressed miRNAs in metastatic CRC. To find miRNAs involved in CRC lymph node metastasis, we first undertook miRNA microarray analysis of submucosal invasive CRC tissues and compared miRNA expression profiles between three non-metastatic and three metastatic CRCs (cases 1–3 and 7–9, respectively; Table S1). The expression levels of miR-125a-5q, miR-125b, miR-155, miR-342-3p, miR-100, and miR-30a-5p were significantly lower in the metastatic CRCs than in the non-metastatic CRCs (Table 1), and the average fold changes were -1.74 , -2.73 , -2.47 , -2.94 , -2.80 , and -2.81 , respectively.

Validation of miRNA expression by qPCR. To validate the differential expression of the six miRNAs, their levels were measured by qPCR in 10 non-metastatic and six metastatic CRC tissues (Table S1). The amounts of miR-100 and miR-125b in the metastatic CRCs were significantly lower than in the non-metastatic CRCs ($P = 0.0092$ and 0.0067 , respectively; Table 2). However, we could not detect significant difference in the expression levels of miR-125a-5q, miR-155, miR342-3p, or miR-30a-5p. Thus, we identified miR-100 and miR-125b as putative miRNAs involved in lymph node metastasis of CRCs with submucosal invasion.

Effects of miRNA inhibitors or mimics on cell invasion. To detect possible roles of miR-100 and miR-125b in malignant phenotypes of colon cancer cells, we first analyzed the

expression of miR-100 and miR-125b in colon cancer cell lines (HT29, SW480, HCT116, RKO, and COLO205) by qPCR. Among the cell lines examined, HCT116 cells expressed moderate amounts of miR-100 and miR-125b that are the most suitable for both knockdown and overexpression experiments (Fig. S1). To test whether altered expression of miR-100 or miR-125b could modify the invasiveness of colon cancer cells, we transfected inhibitors or mimics specific for the two miRNAs in HCT116 cells, and assessed the invasive ability. The invasion of HCT116 cells transfected with a miR-100 or miR-125b inhibitors was significantly higher than that of cells transfected with a miRNA inhibitor negative control (Fig. 1a). In contrast, transfection with a miR-100 or miR-125b mimic significantly reduced cell invasion compared with a negative control mimic (Fig. 1b). We also carried out similar experiments using another CRC cell line, RKO, and obtained similar results on cell invasion (Fig. S2). These results suggest that miR-100 and miR-125b suppress CRC cell invasion. In addition, when both miR-100 and miR-125b inhibitors were simultaneously transfected into HCT116 cells, their invasiveness was slightly more enhanced compared to that of transfectant with each inhibitor alone, despite no significant difference. Likewise, cotransfection of miR-100 and miR-125b mimics into HCT116 cells slightly attenuated their invasiveness compared to transfection with each mimic alone, despite no significant difference (Fig. S3).

Effects of miRNA inhibitors or mimics on migration, cell growth, and MMP activities. Next, we examined the effects of miRNA inhibitors or mimics on HCT116 cell migration. As shown in Figure 2, both miR-100 and miR-125b inhibitors increased HCT116 cell migration and significantly accelerated wound healing compared with control cells. In contrast, the miR-100 and miR-125b mimics significantly impaired wound healing (Fig. 2c,d). When RKO cells were transfected with miR-100 and miR-125b inhibitors or mimics, similar results were obtained on cell migration (Fig. S4). Moreover, we assessed growth promoting activities of miR-100 and miR-125b using the WST-8 assay. As shown in Figure 3, however, silencing and overexpression of miR-100 or miR-125b did not influence HCT116 cell growth. Likewise, silencing of miR-100 or miR-125b did not influence RKO cell growth (Fig. S5). Thus, the reduction of miR-100 or miR125b levels significantly augmented cell invasion and migration without altering their growth rate. We also examined the effects of

Table 1. MicroRNA (miRNA) levels decreased in metastatic colorectal cancer (CRC) compared to non-metastatic CRC

miRNA	Change relative to non-metastatic CRC	<i>P</i> -value†	miRBase accession no.
hsa-miR-125a-5p	-1.77	0.020	MIMAT0000443
hsa-miR-125b	-2.73	0.026	MIMAT0000423
hsa-miR-155	-2.47	0.033	MIMAT0000646
hsa-miR-342-3p	-2.94	0.035	MIMAT0000753
hsa-miR-100	-2.80	0.039	MIMAT0000098
hsa-miR-30a-5p	-2.81	0.042	MIMAT0000087

†Corresponding *P*-values were calculated using unpaired *t*-test.

Table 2. MicroRNA (miRNA) expression in non-metastatic and metastatic colorectal cancers validated by Taqman PCR

miRNA	Mean miRNA expression (relative to RNU48)		<i>P</i> -value‡
	Non-metastatic tumor (<i>n</i> = 10)†	Metastatic tumor (<i>n</i> = 6)†	
hsa-miR-100	1.358 ± 0.414	0.092 ± 0.039	0.0092
hsa-miR-125b	4.631 ± 1.618	0.284 ± 0.131	0.0067
hsa-miR-125a-5p	0.484 ± 0.204	0.162 ± 0.115	0.1585
hsa-miR-155	0.761 ± 0.318	0.682 ± 0.438	0.4477
hsa-miR-342-3p	0.473 ± 0.132	0.451 ± 0.409	0.1289
hsa-miR-30a-5p	2.351 ± 0.921	0.851 ± 0.568	0.2328

†Values are miRNA levels (mean ± SEM) normalized by RNU48 levels.
‡Corresponding *P*-values were calculated using the Mann–Whitney *U*-test.

Fig. 1. Effects of microRNA (miRNA) inhibitors or mimics on cell invasion. (a) HCT116 cells were transfected with miR-100 inhibitor, miR-125b inhibitor, or miRNA inhibitor negative control (Inhibitor-NC), and an invasion assay was carried out. (b) HCT116 cells were transfected with miR-100 mimic, miR-125b mimic, or miRNA mimic negative control (Mimic-NC), and an invasion assay was undertaken. All experiments were carried out six times. * $P < 0.05$; ** $P < 0.01$.

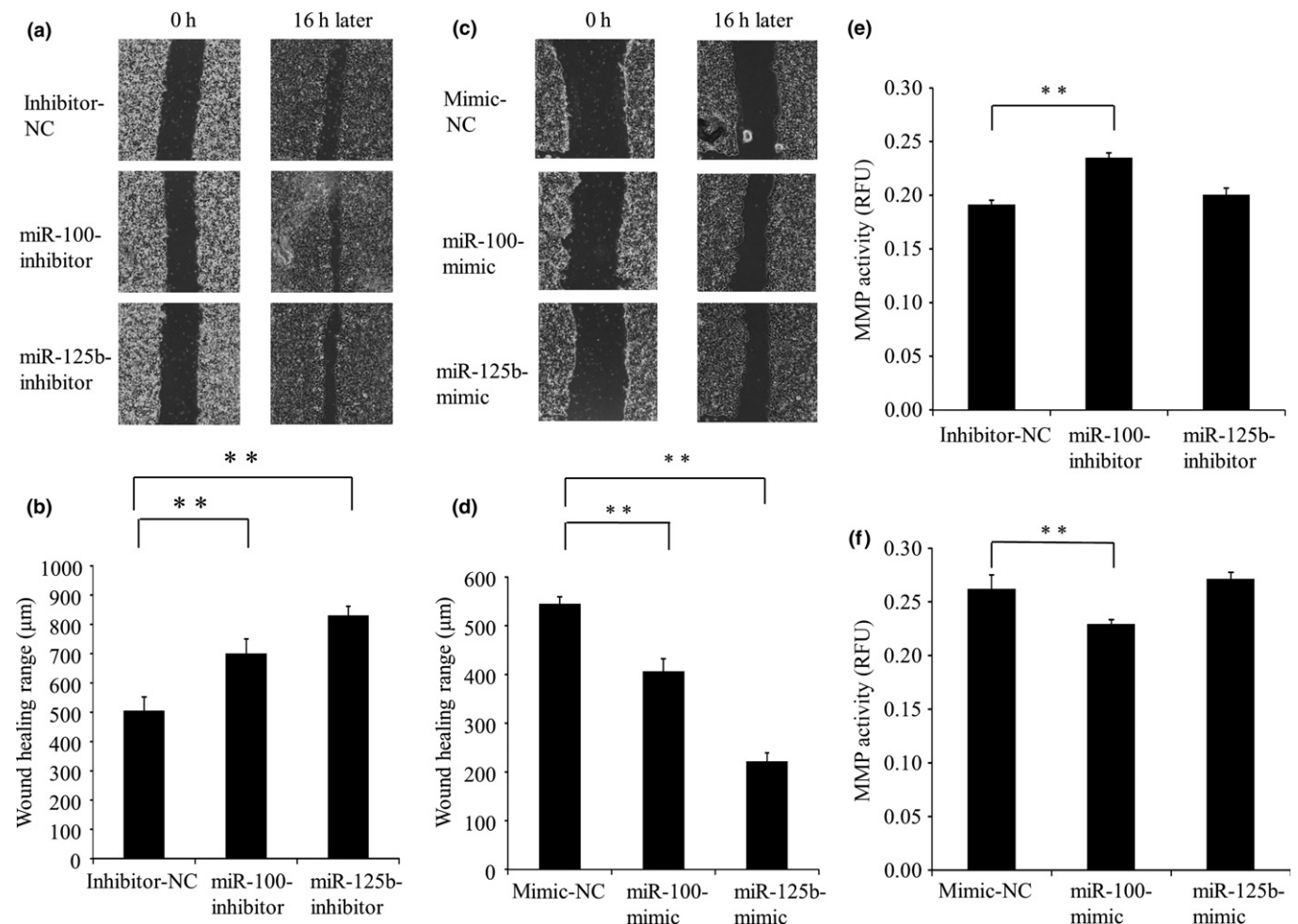
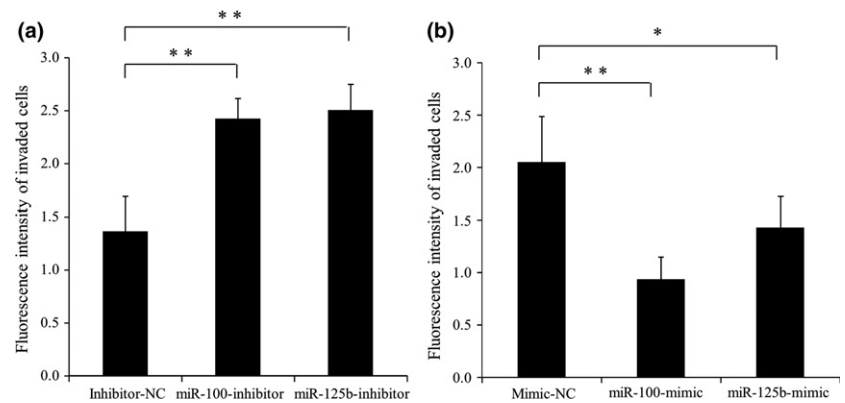


Fig. 2. Effects of microRNA (miRNA) inhibitors or mimics on migration and MMP activities. (a, b) HCT116 cells were transfected with miR-100 inhibitor, miR-125b inhibitor, or miRNA inhibitor negative control (Inhibitor-NC), and a wound healing assay was undertaken. (c, d) HCT116 cells were transfected with miR-100 mimic, miR-125b mimic, or miRNA mimic negative control (Mimic-NC), and a wound healing assay was undertaken. (e) HCT116 cells were transfected with miR-100 inhibitor, miR-125b inhibitor, or miRNA inhibitor negative control (Inhibitor-NC), and an MMP activity assay was undertaken. (f) HCT116 cells were transfected with miR-100 mimic, miR-125b mimic, or miRNA mimic negative control (Mimic-NC), and an MMP activity assay was undertaken. ** $P < 0.01$ versus controls. RFU, relative fluorescence units.

inhibitors or mimics on MMP activities. Silencing of miR-100 significantly increased MMP activities, and miR-100 mimic overexpression significantly reduced those activities (Fig. 2e, f). Instead, neither miR-125 inhibitor nor mimic affected MMP activities (Fig. 2e,f). Thus, miR-100 is likely to be involved in the regulation of both migration and MMP

activities, suggesting that miR-100, rather than miR-125b, may be a possible candidate responsible for the regulation of CRC invasion.

Putative targets. To identify miR-100 target mRNAs involved in cell invasion, we first compared the gene expression profile in miR-100-silenced HCT116 cells with HCT116

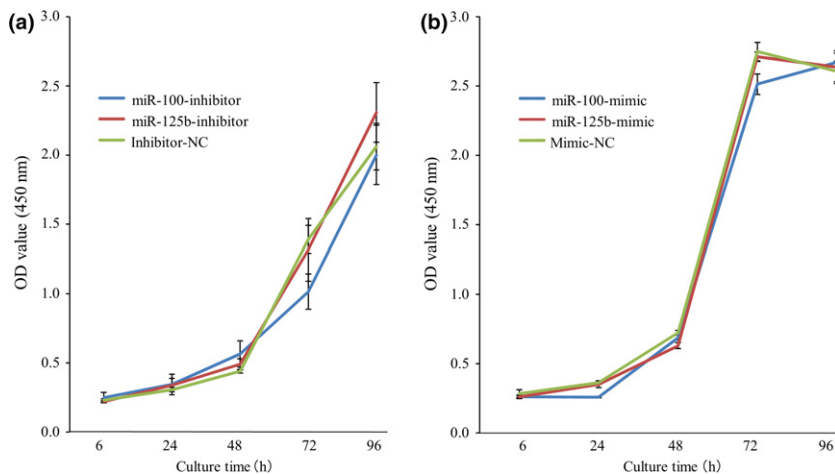


Fig. 3. Effects of microRNA (miRNA) inhibitors or mimics on cell growth. (a) HCT116 cells were transfected with miR-100 inhibitor, miR-125b inhibitor, or miRNA inhibitor negative control (Inhibitor-NC), and a cell proliferation assay was undertaken. (b) HCT116 cells were transfected with miR-100 mimic, miR-125b mimic, or miRNA mimic negative control (Mimic-NC), and a cell proliferation assay was undertaken. OD, optical density.

cells transfected with the miRNA inhibitor negative control. Silencing of miR-100 upregulated and downregulated 54 and 57 genes >1.5-fold, respectively. The 111 differentially expressed genes were subjected to the IPA search. The top five “molecular and cellular functions” related to the differentially expressed genes are listed in Table 3. We also surveyed putative miR-100 target mRNAs. The IPA and TargetScan analyses picked two miR-100 target genes (*mTOR* and *IGF1R*) from the differentially expressed genes, which participate in both “metastasis” and “invasion of cells” (Table 3). The TargetScan analysis indicated that miR-100 directly interacts with *mTOR* and *IGF1R* mRNAs (Fig. S6). The IPA also picked 10 indirect miR-100 target genes (*FAS*, *XIAP*, *PAPPA*, *TFF3*, *SPARC*, *SLC9A1*, *PDLIM3*, *FUT7*, *NCOA1*, and *DKK3*) among the differentially expressed genes, whose functions are related to “metastasis” and/or “invasion of cells” (Table 3). Of these, *FAS*, *XIAP*, and *PAPPA* mRNA levels changed >2-fold after miRNA silencing compared with control cells. Based on these findings, we selected the five genes *mTOR*, *IGF1R*, *Fas*, *XIAP*, and *PAPPA* as candidate targets of miR-100.

Identification of miR-100 targets responsible for cell invasion. To examine whether miR-100 actually controlled the expression of the five genes *mTOR*, *IGF1R*, *Fas*, *XIAP*, and *PAPPA*, we measured changes in expression levels of these mRNAs by qPCR after silencing miR-100 (HCT116/inhibitor) or overexpressing miR-100 (HCT116/mimic). The miR-100 inhibitor significantly increased *mTOR*, *Fas*, *XIAP*, and *IGF1R* mRNA levels (Fig. 4a), whereas the miR-100 mimic significantly decreased them (Fig. 4b), compared with the respective controls. However, *PAPPA* mRNA could not be detected in HCT116 cells transfected with negative controls, inhibitors, or mimics. Similar results were obtained when miR-100 and miR-125b inhibitors or mimics were transfected into RKO cells (Fig. S7).

Finally, to test whether *mTOR*, *Fas*, *XIAP*, and *IGF1R* are involved in the regulation of cell invasion, we examined the effect of siRNA targeting each gene. As shown in Figure 4(c), transfection of the specific siRNA targeting each gene significantly suppressed invasion. In the analysis of cell growth for these transfectants, there were no significant differences between the transfectants and control cells (Fig. S8). Thus, it is evident that *mTOR*, *Fas*, *XIAP*, and *IGF1R* are indeed involved in the regulation of cell invasion.

Discussion

We report here that miR-100 and miR125b are downregulated in early CRCs with lymph node metastasis with submucosal invasion. The expression levels of miR-100 and miR125b were inversely correlated with invasion and migration capabilities of CRC cell lines (HCT116 and RKO) but not with growth-promoting abilities. The levels of miR-100, but not miR-125b, were inversely correlated with MMP activities in HCT116 cells. Finally, we identified *mTOR*, *Fas*, *XIAP*, and *IGF1R* as miR-100 targets, probably involved in the accelerated invasiveness of CRCs with submucosal invasion. In fact, immunohistochemical analysis on the 16 CRC tissues (10 non-metastatic and six metastatic CRCs) revealed that quantitative immunostaining scores for all four these genes in submucosal CRC with lymph node metastasis were significantly higher than in those without lymph node metastasis (Fig. S9). Knockdown of these proteins significantly suppressed the invasion of HCT116 cells. Thus, the present study suggests miR-100 as a useful biomarker for diagnosis and treatment of early CRCs with submucosal invasion.

Yuan *et al.*⁽¹⁵⁾ reported the increased expression of miR-145 in CRC with lymph node metastasis. They also showed that miR-100 and miR-125b levels in CRC tissues with lymph node metastasis are significantly higher than in CRCs without lymph node metastasis, thus contradicting our results. In our miRNA microarray analysis, miR-145 levels were decreased in submucosal invasive CRCs with lymph node metastasis compared with CRCs without lymph node metastasis. They examined miR-145 expression in CRCs with and without lymph node metastasis from stage I to stage IV (mainly stage III). In contrast, we enrolled patients with early stage CRCs with limited invasion to the submucosal layer. The size of the tumors examined in our study ranged from 10 to 20 mm in diameter, and there was no significant difference in the size of the lesion in cases with and without lymph node metastasis. Therefore, our samples may be suitable for analysis of miRNAs participating in lymph node metastasis in the early stages of CRC. Consistent with our findings, it has been reported that miR-100 and miR-125b levels are significantly lower in metastatic prostate cancer and osteosarcoma, respectively.^(21,22)

Of the four genes identified as miR100 targets (*mTOR*, *Fas*, *XIAP*, and *IGF1R*), *mTOR*, a downstream member of the phosphoinositide 3-kinase/Akt/mTOR pathway, is known as a central regulator of cell growth and differentiation. Recently,

Table 3. Ingenuity pathway analysis and TargetScan analyses of 111 differentially expressed genes in HCT116 cells treated with a microRNA-100 (miR-100) inhibitor

Functions	Related genes	P-values†
Direct target of miR-100 related with “invasion of cells” and “metastasis”	<i>MTOR</i> ↑, <i>IGF1R</i> ↑	
Indirect target of miR-100 related with “invasion of cells” and/or “metastasis”	<i>Fas</i> ↑, <i>XIAP</i> ↑, <i>PAPPA</i> ↓, <i>TFF3</i> ↑, <i>PDLIM3</i> ↓, <i>FUT7</i> ↓, <i>NCOA1</i> ↓, <i>SPARC</i> ↑, <i>SLC9A1</i> ↑, <i>DKK3</i> ↓	
Top 5 molecular and cellular functions		
1. Cell death and survival	<i>Fas</i> ↑, <i>NR5A2</i> ↑, <i>TFF3</i> ↑, <i>IL21</i> ↑, <i>TRAF1</i> ↓, <i>NR4A3</i> ↓, <i>SH3BP2</i> ↓, <i>XIAP</i> ↑, <i>SLC4A1</i> ↓, <i>SFTPC</i> ↑, <i>TSC1</i> ↓, <i>SPARC</i> ↑, <i>NCOA1</i> ↓, <i>SLC8A1</i> ↓, <i>HSPB6</i> ↓, <i>SLC9A1</i> ↑, <i>CSHL1</i> ↓, <i>GPR37L1</i> ↑, <i>DKK3</i> ↓, <i>ORAI1</i> ↑, <i>CHAT</i> ↑, <i>PAX4</i> ↑	4.14E-05
2. Cellular compromise	<i>Fas</i> ↑, <i>IL21</i> ↑, <i>SLC9A1</i> ↑, <i>SLC4A1</i> ↓, <i>SPARC</i> ↑, <i>SH3BP2</i> ↓, <i>XIAP</i> ↑, <i>ORAI1</i> ↑, <i>TSC1</i> ↓	2.83E-04
3. Cellular function and maintenance	<i>SLC8A1</i> ↓, <i>SLC9A1</i> ↑, <i>IL21</i> ↑, <i>SH3BP2</i> ↓, <i>FCN1</i> ↑, <i>Fas</i> ↑, <i>SLC4A1</i> ↓, <i>SLC9A1</i> ↑, <i>GORASP1</i> ↓, <i>CHAT</i> ↑, <i>SEC16A</i> ↓, <i>ORAI1</i> ↑, <i>TSC1</i> ↓, <i>CDKL5</i> ↑, <i>MAP6</i> ↓	4.23E-04
4. Molecular transport	<i>SLC8A1</i> ↓, <i>SLC9A1</i> ↑, <i>SLC26A11</i> ↓, <i>SLC4A1</i> ↓, <i>Fas</i> ↑, <i>NR5A2</i> ↑, <i>PITPNC1</i> ↓, <i>CHRN4</i> ↑, <i>CLCC1</i> ↑, <i>KCNQ5</i> ↑, <i>TSC1</i> ↓, <i>PGAP1</i> ↓, <i>CSHL1</i> ↓, <i>MTR</i> ↑, <i>C1QTNF5</i> ↓, <i>CHAT</i> ↑, <i>FOLR3</i> ↓, <i>NR4A3</i> ↓, <i>SEC13</i> ↓, <i>KCNQ5</i> ↑	4.23E-04
5. Small molecule biochemistry	<i>SLC8A1</i> ↓, <i>SLC9A1</i> ↑, <i>Fas</i> ↑, <i>MTR</i> ↑, <i>OBP2B</i> ↓, <i>NR5A2</i> ↑, <i>PITPNC1</i> ↓, <i>NCOA1</i> ↓, <i>SLC4A1</i> ↓, <i>PGAP1</i> ↓, <i>CSHL1</i> ↓, <i>POFUT1</i> ↓	4.23E-04

↑, upregulated gene; ↓, downregulated gene. †Calculated by Fisher's exact test.

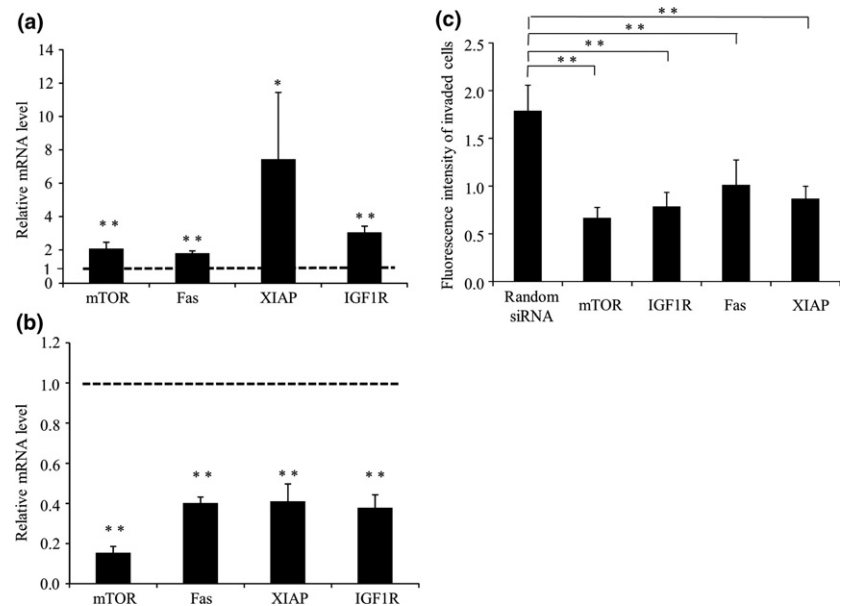


Fig. 4. Identification of microRNA (miR)-100 targets responsible for cell invasion. (a, b) Changes in the expression levels of five genes *mTOR*, *IGF1R*, *Fas*, *XIAP*, and *PAPPA* were measured by quantitative PCR after silencing (a, HCT116/inhibitor) or after overexpressing miR-100 (b, HCT116/mimic). (c) HCT116 cells were transfected with a random siRNA or the siRNA targeting *mTOR*, *Fas*, *XIAP*, or *IGF1R*, and an invasion assay was carried out. * $P < 0.05$; ** $P < 0.01$ versus controls.

mTOR has been reported to play a pivotal role in metastasis of cancer cells through enhanced motility and invasiveness, E-cadherin downregulation, and MMP-2 upregulation.^(23,24) Thus, it is highly plausible that downregulated miR-100 promotes lymph node metastasis through *mTOR*. The IGF1 receptor plays a critical role in carcinogenesis. Recently, Li et al.⁽²⁵⁾ reported that IGF1/IGF1R signaling induces tumor-associated lymphangiogenesis and contributes to lymphatic metastasis in advanced CRCs. Our results suggest that IGF1R may play an important role in lymph node metastasis, even in early CRCs with submucosal invasion. Fas/FasL signaling is well known to be a crucial mediator of cell apoptosis. However, Zheng et al.⁽²⁶⁾ indicated that low-dose Fas stimulation induced epithelial–mesenchymal transition to promote tumor motility and metastasis in gastrointestinal cancer *in vivo* and *in vitro*. Therefore, it is possible that persistent weak Fas signals may stimulate lymph node metastasis in early CRCs with

submucosal invasion. An inhibitor of apoptosis, XIAP, is overexpressed in various types of cancers.⁽²⁷⁾ Shi et al.⁽²⁸⁾ reported that XIAP was closely associated with metastatic capability, invasiveness, and resistance to apoptosis in hepatocellular carcinoma cells. Upregulated XIAP may be involved in lymph node metastasis in submucosal invasive CRCs. Thus, all four miR-100 target genes (*mTOR*, *IGF1R*, *Fas*, and *XIAP*) may promote lymph node metastasis in submucosal invasive CRCs.

Eventually, in order to identify miR-125b target mRNAs, we also compared the gene expression profile in miR-125b-silenced HCT116 cells and control cells. We found 16 differentially expressed genes (>1.5-fold). The IPA and TargetScan analyses of these genes picked one gene, *XIAP*. The TargetScan analysis indicated that miR-125b may interact with *XIAP*. The IPA did not pick any other indirect target genes among these genes whose functions are related to “metastasis” and/or “invasion” of cells. Thus, downregulation of miR-125b may

promote lymph node metastasis by upregulating *XIAP* and/or other unknown target genes. A more detailed analysis of miR-125b targets should be investigated in the future.

One limitation of our study is the relatively small number of clinical samples examined. The prevalence of lymph node metastasis is low (only approximately 10%) in CRC with submucosal invasion. Therefore, it is difficult to obtain sufficient numbers of CRC samples with lymph node metastasis.⁽²⁾ It would be necessary to investigate the expression of miR-100, miR-125b expression, and target genes in a large number of CRC specimens with submucosal invasion with and without lymph node metastasis as a multicenter study.

In conclusion, our study shows that downregulation of miR-100 and miR-125b is closely associated with lymph node metastasis in early CRC with intrasubmucosal invasion through enhancement of invasion, motility, and MMP activity. In particular, downregulation of miR-100 may promote lymph node metastasis by upregulating mTOR and IGF1R as direct targets, and Fas and XIAP as indirect targets. Thus, miR-100 and miR-125b may be novel biomarkers for lymph node metastasis of early CRCs with submucosal invasion.

Acknowledgments

We thank Katsutaka Sannomiya (Department of Gastroenterology and Oncology, Institute of Biomedical Sciences, Tokushima University Graduate School) and Hideaki Horikawa (Support Center for Advanced Medical Sciences, Institute of Biomedical Sciences, Tokushima University Graduate School) for valuable advice. This work was supported by the Japan Society for the Promotion of Science (Kakenhi grant no. 15K09059) and the Japanese Foundation for Research and Promotion of Endoscopy.

Disclosure Statement

The authors have no conflict of interest.

Abbreviations

CRC	colorectal cancer
IGF1R	insulin-like growth factor 1 receptor
IPA	Ingenuity Pathway Analysis
miRNA	microRNA
mTOR	mammalian target of rapamycin
qPCR	quantitative PCR
XIAP	X-linked inhibitor-of-apoptosis protein

References

- 1 Tanaka S, Oka S, Chayama K. Colorectal endoscopic submucosal dissection: present status and future perspective, including its differentiation from endoscopic mucosal resection. *J Gastroenterol* 2008; **43**: 641–51.
- 2 Kitajima K, Fujimori T, Fujii S *et al*. Correlations between lymph node metastasis and depth of submucosal invasion in submucosal invasive colorectal carcinoma: a Japanese collaborative study. *J Gastroenterol* 2004; **39**: 534–43.
- 3 Watanabe T, Itabashi M, Shimada Y *et al*. Japanese Society for Cancer of the Colon and Rectum (JSCCR) Guidelines 2014 for treatment of colorectal cancer. *Int J Clin Oncol* 2015; **20**: 207–39.
- 4 Pimentel-Nunes P, Dinis-Ribeiro M, Ponchon T *et al*. Endoscopic submucosal dissection: European Society of Gastrointestinal Endoscopy (ESGE) Guideline. *Endoscopy* 2015; **47**: 829–54.
- 5 Fisher DA, Shergill AK, Early DS, Comm ASP. Role of endoscopy in the staging and management of colorectal cancer (vol 78, pg 8, 2013). *Gastrointest Endosc* 2013; **78**: 559.
- 6 Lagos-Quintana M, Rauhut R, Lendeckel W, Tuschl T. Identification of novel genes coding for small expressed RNAs. *Science* 2001; **294**: 853–8.
- 7 Lau NC, Lim LP, Weinstein EG, Bartel DP. An abundant class of tiny RNAs with probable regulatory roles in *Caenorhabditis elegans*. *Science* 2001; **294**: 858–62.
- 8 Lee RC, Ambros V. An extensive class of small RNAs in *Caenorhabditis elegans*. *Science* 2001; **294**: 862–4.
- 9 Guo H, Ingolia NT, Weissman JS, Bartel DP. Mammalian microRNAs predominantly act to decrease target mRNA levels. *Nature* 2010; **466**: 835–40.
- 10 Bazzini AA, Lee MT, Giraldez AJ. Ribosome profiling shows that miR-430 reduces translation before causing mRNA decay in zebrafish. *Science* 2012; **336**: 233–7.
- 11 Calin GA, Croce CM. MicroRNA signatures in human cancers. *Nat Rev Cancer* 2006; **6**: 857–66.
- 12 Croce CM. Causes and consequences of microRNA dysregulation in cancer. *Nat Rev Genet* 2009; **10**: 704–14.
- 13 Mestdagh P, Hartmann N, Baeriswyl L *et al*. Evaluation of quantitative miRNA expression platforms in the microRNA quality control (miRQC) study. *Nat Methods* 2014; **11**: 809–15.
- 14 Li W, Chang J, Wang S *et al*. miRNA-99b-5p suppresses liver metastasis of colorectal cancer by down-regulating mTOR. *Oncotarget* 2015; **6**: 24448–62.

- 15 Yuan W, Sui C, Liu Q, Tang W, An H, Ma J. Up-regulation of microRNA-145 associates with lymph node metastasis in colorectal cancer. *PLoS ONE* 2014; **9**: e102017.
- 16 Li Y, Liu J, Fan Y *et al*. Expression levels of microRNA-145 and microRNA-10b are associated with metastasis in non-small cell lung cancer. *Cancer Biol Ther* 2016; **17**: 272–9.
- 17 Wang M, Wang J, Deng J, Li X, Long W, Chang Y. MiR-145 acts as a metastasis suppressor by targeting metadherin in lung cancer. *Med Oncol* 2015; **32**: 344.
- 18 Kurokawa K, Akaike Y, Masuda K *et al*. Downregulation of serine/arginine-rich splicing factor 3 induces G1 cell cycle arrest and apoptosis in colon cancer cells. *Oncogene* 2014; **33**: 1407–17.
- 19 Qian L, Xie B, Wang Y, Qian J. Amygdalin-mediated inhibition of non-small cell lung cancer cell invasion in vitro. *Int J Clin Exp Pathol* 2015; **8**: 5363–70.
- 20 Zeng Y, Adamson RH, Curry F-RE, Tarbell JM. Sphingosine-1-phosphate protects endothelial glycocalyx by inhibiting syndecan-1 shedding. *Am J Physiol Heart Circ Physiol* 2014; **306**: H363–72.
- 21 Leite KRM, Sousa-Canavez JM, Reis ST *et al*. Change in expression of miR-let7c, miR-100, and miR-218 from high grade localized prostate cancer to metastasis. *Urol Oncol* 2011; **29**: 265–9.
- 22 Karbasy SH, Taheriazam A, Mirghasemi A *et al*. Upregulation of miR-300 and downregulation of miR-125b act as potential predictor biomarkers in progression, metastasis, and poor prognosis of osteosarcoma. *Tumour Biol* 2015; **36**: 1–5.
- 23 Niu P-G, Zhang Y-X, Shi D-H, Liu Y, Chen Y-Y, Deng J. Cardamonin inhibits metastasis of Lewis lung carcinoma cells by decreasing mTOR activity. *PLoS ONE* 2015; **10**: e127778.
- 24 Ye Z, Al-aidaroos AQO, Park JE *et al*. PRL-3 activates mTORC1 in cancer progression. *Sci Rep* 2015; **5**: 17046.
- 25 Li Z-J, Ying X-J, Chen H-L *et al*. Insulin-like growth factor-1 induces lymphangiogenesis and facilitates lymphatic metastasis in colorectal cancer. *World J Gastroenterol* 2013; **19**: 7788–94.
- 26 Zheng HX, Cai YD, Wang YD *et al*. Fas signaling promotes motility and metastasis through epithelial-mesenchymal transition in gastrointestinal cancer. *Oncogene* 2013; **32**: 1183–92.
- 27 Deveraux QL, Takahashi R, Salvesen GS, Reed JC. X-linked IAP is a direct inhibitor of cell-death proteases. *Nature* 1997; **388**: 300–4.
- 28 Shi Y-H, Ding W-X, Zhou J *et al*. Expression of X-linked inhibitor-of-apoptosis protein in hepatocellular carcinoma promotes metastasis and tumor recurrence. *Hepatology* 2008; **48**: 497–507.

Supporting Information

Additional Supporting Information may be found online in the supporting information tab for this article:

Fig. S1. MicroRNA (miR)-100 and miR-125b expression in various colorectal cancer cell lines. Relative miR-100 (a) or miR-125b (b) expression levels in HT-29, COLO205, SW480, HCT116, and RKO cells were measured by TaqMan real-time PCR. RNU48 was used as an internal control.

Fig. S2. Effects of microRNA (miRNA) inhibitors or mimics on cell invasion. (a) RKO cells were transfected with miR-100 inhibitor, miR-125b inhibitor, or miRNA inhibitor negative control (Inhibitor-NC), and an invasion assay was undertaken. (b) RKO cells were transfected with miR-100 mimic, miR-125b mimic, or miRNA mimic negative control (Mimic-NC), and an invasion assay was undertaken. All experiments were carried out six times. * $P < 0.05$; ** $P < 0.01$.

Fig. S3. Combined effects of microRNA (miR)-100 and miR-125b inhibitors or mimics on cell invasion. (a) HCT116 cells were transfected with miR-100 inhibitor, miR-125b inhibitor, miR-100 inhibitor + miR-125b inhibitor or miRNA inhibitor negative control (Inhibitor-NC), and an invasion assay was undertaken. (b) HCT116 cells were transfected with miR-100 mimic, miR-125b mimic, miR-100 mimic + miR-125b mimic or miRNA mimic negative control (Mimic-NC), and an invasion assay was undertaken. * $P < 0.05$; ** $P < 0.01$.

Fig. S4. Effects of microRNA (miRNA) inhibitors or mimics on migration. (a, b) RKO cells were transfected with miR-100 inhibitor, miR-125b inhibitor, or miRNA inhibitor negative control (Inhibitor-NC), and a wound healing assay was carried out. (c, d) RKO cells were transfected with miR-100 mimic, miR-125b mimic, or miRNA mimic negative control (Mimic-NC), and a wound healing assay was carried out. ** $P < 0.01$.

Fig. S5. Effects of microRNA (miRNA) inhibitors on cell growth. RKO cells were transfected with miR-100 inhibitor, miR-125b inhibitor, or miRNA inhibitor negative control (Inhibitor-NC), and a cell proliferation assay was carried out. OD, optical density.

Fig. S6. Predicted consequential pairing of microRNA (miR)-100 and the target regions of mammalian target of rapamycin (mTOR) and insulin-like growth factor 1 receptor (IGF1R). The TargetScan analysis revealed that miR-100 directly interacts with mTOR and IGF1R mRNAs; miR-100 possesses complementary matches to sequences within the 3'-UTRs of mTOR (position 295–301). Likewise, miR-100 represents complementary matches to sequences within the 3'-UTRs of IGF1R (position 5602–5609).

Fig. S7. Identification of microRNA (miR)-100 targets responsible for cell invasion. (a, b) Changes in the expression levels of the five genes *mTOR*, *IGF1R*, *Fas*, *XIAP*, and *PAPPA* were measured by quantitative PCR after silencing (a, RKO/inhibitor) or after overexpressing miR-100 (b, RKO/mimic). * $P < 0.05$; ** $P < 0.01$ versus controls.

Fig. S8. Effects of siRNA for mammalian target of rapamycin (mTOR), Fas, X-linked inhibitor-of-apoptosis protein (XIAP), or insulin-like growth factor 1 receptor (IGF1R) on cell growth. (a) HCT116 cells were transfected with random siRNA or siRNA for mTOR, Fas, XIAP or IGF1R, and a cell proliferation assay was carried out. No statistically significant differences in cell growth were observed between the transfectants of the siRNA for mTOR, Fas, XIAP, or IGF1R, or of random siRNA. OD, optical density. (b) Relative mRNA levels for mTOR, Fas, XIAP, and IGF1R were measured by quantitative PCR at 48 h to validate knockdown efficiency of these genes. Representative data at 48 h are shown. ** $P < 0.01$ versus controls.

Fig. S9. Immunohistochemical staining for mammalian target of rapamycin (mTOR), insulin-like growth factor 1 receptor (IGF1R), Fas, and X-linked inhibitor-of-apoptosis protein (XIAP) in colorectal cancer (CRC) tissue. Immunohistochemical staining was carried out using the labeled streptavidin–biotin method with rabbit anti-human mTOR antibody (ab2732), rabbit anti-human IGF-1R antibody (bs-0227R), rabbit anti-human Fas antibody (119-16559), or rabbit anti-human XIAP antibody (ab21278). (a, b) mTOR, (c, d) IGF1R, (e, f) Fas, and (g, h) XIAP in CRC tissues without lymph node (LN) metastasis ($\times 100$) and with LN metastasis ($\times 100$). Scores for percentage of positive cells were assigned as follows: 0, $\leq 10\%$ of cells positive; 1, 11–25% of cells positive; 2, 26–50% of cells positive; 3, 51–75% of cells positive; and 4, $> 75\%$ of cells positive. Scores for staining intensity were assigned as follows: 0, no staining; 1, light brown; 2, brown; and 3, dark brown. Overall scores were obtained by multiplying the percentage score by the intensity score. The Mann–Whitney *U*-test was used to assess difference in immunohistochemical score between human CRC tissues with and without lymph node metastasis. IQR, interquartile range.

Table S1. Baseline characteristics of the patients who participated in this study. We undertook microRNA (miRNA) microarray analysis of sub-mucosal invasive colorectal cancer (CRC) tissues and compared miRNA expression profiles between three non-metastatic (cases 1–3) and three metastatic (cases 7–9) CRCs. To validate the differential expression of the six miRNAs, their levels were measured by quantitative PCR in 10 non-metastatic and six metastatic CRC tissues (cases 1–16).